

Atomistic Simulation Study of the Coupled Motion of Amino Acid Residues and Water Molecules around Protein HP-36: Fluctuations at and around the Active Sites

Sanjoy Bandyopadhyay,^{*,†} Sudip Chakraborty,[†] Sundaram Balasubramanian,[‡] Subrata Pal,[§] and Biman Bagchi^{*,§}

Molecular Modeling Laboratory, Department of Chemistry, Indian Institute of Technology, Kharagpur 721302, India, Chemistry and Physics of Materials Unit, Jawaharlal Nehru Centre for Advanced Scientific Research, Jakkur, Bangalore 560064, India, and Solid State and Structural Chemistry Unit, Indian Institute of Science, Bangalore 560012, India

Received: April 3, 2004; In Final Form: June 19, 2004

The chicken villin headpiece subdomain, popularly known as HP-36, is an actin binding protein. It consists of 36 amino acid residues in three α -helices and four coils. The biological activity of the protein is found to be centered around helix-3, which contains 10 amino acid residues. We have performed atomistic molecular dynamics simulations of HP-36 with explicit water in order to investigate the correlation, if any, between the dynamics of the amino acid residues, dynamics of surrounding water molecules, and the biological activity of the protein. We calculate the time trajectory of the root mean square deviation (RMSD) of *individual* amino acid residues, the rotational and translational motion of water molecules, and the dynamics of hydrogen bonds formed between the protein residues and the interfacial water molecules near different segments of HP-36. We find that the amino acid residues in the short helices 1 and 2 exhibit no interesting dynamics; the time trajectory of their RMSD shows only minor changes with time. In contrast, the residues in helix-3 (the biologically active one) show highly interesting dynamics, often exhibiting large amplitude, sometimes nearly oscillatory motions. Simultaneously, the water molecules near helix-3 are found to exhibit noticeably faster rotational and translational motions. It has been observed that the structural relaxation of the hydrogen bonds formed between the residues in helix-3 and the interfacial water molecules is faster than that for the other two helices. Analysis of the structural arrangement of water molecules around the protein in terms of the radial distribution function shows that not only are there fewer water molecules around helix-3 but they are also less structured than those around helices 1 and 2. This is somewhat surprising because the third helix contains several hydrophilic groups. Analysis of the structure of the protein shows that few polar hydrophilic residues remain buried within the core of the protein, which partly explains the lack of structure of water molecules around helix-3.

1. Introduction

A molecular level understanding of the biological activity of a given protein is a goal that is hard to achieve and highly sought after. This area of research offers a classic example of interdisciplinary research, which involves both theoretical and experimental approaches in chemistry, physics, and biology.^{1–8} It is known that the biological activity of a protein is uniquely tied to its native three-dimensional structure. Except for very small proteins, the time-averaged structure of a protein in solution obtained by NMR is the same as the one obtained from X-ray diffraction analysis of protein crystals. This structure itself holds the key to many aspects of the function of the protein. However, to perform this biological activity, such as ligand binding, the protein must undergo certain critical dynamical motions. The time scales of these motions may determine the reaction pathways and also the rate. Since most of the known proteins function in water, it is natural to expect the water molecules surrounding the protein also to participate in the dynamical events that lead to activity. A microscopic level

understanding of the dynamical coupling between the protein and the “biological water” is crucial for many biological processes such as protein–enzyme interactions, molecular recognition, and folding–unfolding phenomena. Because of the importance of the issues involved, this area is currently a subject of intense research.^{7–18} However, the characteristic time scales of the motions involving a solvated protein could range from tens of femtoseconds to milliseconds. Notable advances have been made in laser spectroscopic techniques in studying the time scales associated with different motions. Fleming and co-workers^{7,10} studied the dynamics of protein solvation using three-pulse photon echo shift (3PEPS) techniques. They observed the presence of an ultrafast (<200 fs) as well as a long time scale solvation (>150 ps) of eosin in lysozyme in aqueous solution. Bhattacharyya and co-workers^{8,12,19} have done significant work in this area using time-resolved fluorescence emission spectroscopy with picosecond resolution. They observed the solvation dynamics of a fluoroprobe DCM bound to HSA (human serum albumin) to be biexponential, with a slow (600 ps) and a very long (10 ns) relaxation component. This indicates a restricted movement of water close to the protein molecule. Most of these latter studies have been carried out at picosecond or nanosecond time resolution. However, to probe the local dynamics of the protein, one should study at femtosecond

* To whom correspondence should be addressed. For S.B.: e-mail, sanjoy@chem.iitkgp.ernet.in. For B.B.: e-mail, bbagchi@sscu.iisc.ernet.in.

[†] Indian Institute of Technology.

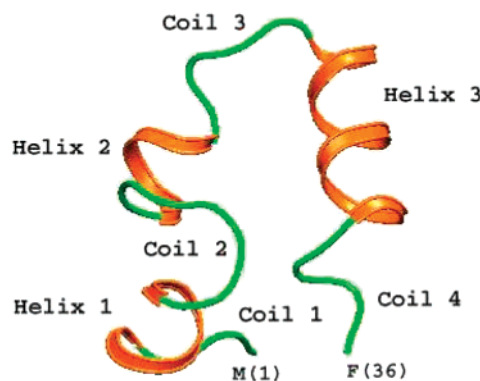
[‡] Jawaharlal Nehru Centre for Advanced Scientific Research.

[§] Indian Institute of Science.

resolution. Recently, Pal et al.^{17,18} have studied the solvation of several proteins with time-resolved fluorescence emission spectroscopy with femtosecond resolution, using tryptophan (Trp) as an intrinsic probe. They found the solvation dynamics of tryptophan to proceed at late stage, with a time constant in the range 20–40 ps, which is about an order of magnitude larger than that for the bulk water. Thus, one may attribute at least a part of the slow dynamics to the slowness of water at the protein surface, although some of the longer time constants reported must also involve contributions from the protein side chain motions. However, there does not appear to exist any study on the relative importance of protein side chain motions in solvation dynamics. We are also not aware of any study of the correlation between the protein side chain motion and water dynamics in the hydration layer. Even more, there are only a few studies that relate the structure and dynamics of water near an active site to its function.

Computer simulation studies can help answer many of the detailed questions regarding the time scale and the nature of the dynamics near a protein surface at a microscopic level. Such studies can help us gain an understanding of the coupling between the protein and solvent dynamics and its likely influence on biological processes. It is now more than a quarter of a century since Karplus and co-workers^{3,20} showed from their early molecular dynamics (MD) simulation studies that proteins are highly dynamical systems with the atoms exhibiting fluid-like motions with significant amplitudes about their mean positions. Today, with the availability of fast computers along with the development of advanced simulation methodologies, one can routinely simulate a moderately sized protein with explicit water molecules for tens of nanoseconds. Although one is still rather far from simulating, atomistically, a full biological event running often into seconds, a lot of microscopic information can now be extracted from nanoseconds-long simulations. There have been several attempts over recent years to study the dynamical properties of protein solutions using simulation methods.^{21–31} These studies have revealed many interesting aspects. Cannistraro and co-workers^{21,22} studied in detail the microscopic dynamical behavior of water near a protein surface. They observed that besides exhibiting highly restricted mobility, the hydration water also show a sublinear trend with time for their mean square displacements, suggesting the existence of anomalous diffusion. Tarek and Tobias^{23–25} have reported water mobility for several proteins in solution as well as in their crystals and dry and hydrated powders, using a combination of MD simulations and quasielastic neutron scattering measurements. They have shown that a complete exchange of protein-bound water molecules is necessary for the structural relaxation of a protein. Recently, Marchi et al.²⁶ have carried out long MD simulations to study the dynamical properties of water near the surface of lysozyme. From a series of MD simulations, Xu and Berne²⁷ have shown that the kinetics of the water–water hydrogen bond formation and breaking in the first solvation shell of a polypeptide is slower than that in bulk water. Pettitt and co-workers^{28–30} have reported extensive MD studies on protein solvation. They employed three-dimensional probability distributions to describe most of the hydration and solvation phenomena for such macromolecules. A nice example of correlation between protein fluctuation and biological activity has been shown by Zhou et al.³² In a notable study, Duan and Kollman³³ simulated the folding of HP-36 in a fully atomistic MD simulation that was 1 μ s long.

There appears to have been relatively less effort directed at establishing a microscopic relationship between biological



MLSDDEDFKAVFGMTRSAFANLPLWKQNLKKEKGLF

Figure 1. Ribbon diagram of the native state structure of the 36-residue villin headpiece subdomain, HP-36, as obtained from NMR data.³⁸ The secondary structures contain three α -helices and four coils (as defined in the text). The α -helices are drawn in red, while the coils are in green. The sequence of the protein is also displayed in one-letter code, with the N-terminus residue M(1) on the left and the C-terminus residue F(36) on the right.

activity and protein dynamics. It seems natural to expect that both the protein side chains and the surrounding water molecules will play an important role in many activities of the protein, such as ligand binding. It is believed that biological activity involves transitions between different conformational substates of a protein,³⁴ which in the modern language could be attributed to different free energy minima near the bottom of the folding funnel.^{35–37} Recently, an atomistic molecular dynamics study of the pathogenic strain of enterotoxin, the 13-amino acid long polypeptide known as 1ETN, was carried out.³¹ It was found that the region active in binding exhibits faster water dynamics. However, no study of the motion of the protein side chains was carried out.

In this article, we report MD simulation studies of both protein and water dynamics of a small 36-residue globular protein, which is the thermostable subdomain present at the extreme C-terminus of the 76-residue chicken villin headpiece domain, popularly known as HP-36.³⁸ Villin is a unique protein that can both assemble and disassemble actin structures.^{39,40} In the absence of calcium ions, it can act as an actin-bundling protein, while in the presence of calcium it becomes an actin-severing protein. HP-36 contains one of the two F-actin binding sites in villin necessary for F-actin bundling activity.³⁹ In this work we number the residues from 1 to 36. Thus, residue numbers 1–36 correspond to residues 41–76 in the NMR structure.^{38,41} The secondary structure of the protein contains three short α -helices. These helices are connected and held together by a few turns and loops and a hydrophobic core. We denote the three α -helices as helix-1 (Asp-4 to Lys-8), helix-2 (Arg-15 to Phe-18), and helix-3 (Leu-23 to Glu-32). The remaining segments of the protein are defined as coil-1 (Met-1 to Ser-3), coil-2 (Ala-9 to Thr-14), coil-3 (Ala-19 to Pro-22), and coil-4 (Lys-33 to Phe-36). The amino acid sequence and the native state structure of the protein as obtained from NMR studies³⁸ are displayed in Figure 1, where we have also marked the α -helices and the coils. The biological activity is believed to be centered around helix-3, which contains 10 amino acid residues.³⁸

2. System Setup and Simulation Details

We have employed a recently developed molecular dynamics package (PINY-MD)⁴² to perform the classical atomistic mo-

lecular dynamics simulations presented in this article. The CHARMM22 all-atom force field and potential parameters for proteins⁴³ were employed to describe the interaction between protein atoms, while the TIP3P model,⁴⁴ which is consistent with the chosen protein force field, was employed for modeling water.

The initial coordinates of the protein were taken from the Protein Data Bank (PDB code: 1VII) from the NMR structure of the villin headpiece subdomain, as reported by McKnight et al.³⁸ The two end residues (Met-1 and Phe-36) of the protein were capped appropriately, and the whole molecule was immersed in a large cubic box of well-equilibrated water. To avoid any unfavorable contact, the insertion process was carried out by carefully removing all the water molecules that were within 2 Å from any atom of the protein molecule. The final system contained the 36-residue-long protein molecule (596 atoms) in a cubic box containing 6842 water molecules. The initial edge length of the cubic simulation cell was 61 Å.

At first, the system was equilibrated at constant temperature ($T = 300$ K) and pressure ($P_{\text{ext}} = 0$) (NPT) for about 500 ps. During this run, the volume of the simulation cell was allowed to fluctuate isotropically. At the end of this equilibration run, the volume of the system attained a steady value with a box edge length of 58.92 Å, and the average pressure of the system was 3 atm. At this point we fixed the cell volume, and the simulation conditions were changed from constant pressure and temperature (NPT) to constant volume and temperature (NVT). The NVT equilibration run was further continued at 300 K for another 1 ns duration. This equilibration period was followed by an NVT production run of approximately 2.5 ns duration. The MD trajectory was stored during the NVT run with a time resolution of 400 fs for subsequent analysis. The time evolution of the root mean square deviation (RMSD) values were calculated over the entire 3.5 ns NVT trajectory, while the other quantities were calculated by averaging over the last 2.5 ns of the equilibrated trajectory.

The simulations utilized the Nosé–Hoover chain thermostat extended system method.⁴⁵ The use of a reversible multiple time step algorithm, RESPA,⁴⁵ allowed us to employ an MD time step of 4 fs. Electrostatic interactions were calculated by using the particle-mesh Ewald (PME) method.⁴⁶ The PME and RESPA were combined following the method suggested by Marchi and co-workers.^{47,48} The minimum image convention⁴⁹ was employed to calculate the Lennard-Jones interactions and the real-space part of the Ewald sum, using a spherical truncation of 7 and 10 Å, respectively, for the short- and the long-range parts of the force decomposition. In the following, we discuss the results.

3. Results and Discussion

3.1. Structure and Dynamics of the Protein. In Figure 2 we display several snapshots of the secondary structure of the protein obtained from the simulation at different time intervals after the equilibration run. The native structure of HP-36 as obtained from NMR experiments³⁸ is also shown for comparison. It is evident from the snapshots that the simulated structure of the protein in solution is significantly similar to the NMR structure. Minor differences were observed between the simulated and the experimental structures, particularly near the terminal residues (coil-1 and coil-4). Figure 3 shows the superposition of the backbone atoms (N, C, and C $_{\alpha}$) of the protein molecule from several configurations taken at a regular interval of about 200 ps from the equilibrated simulation trajectory. The figure indicates that on the whole, the nonter-

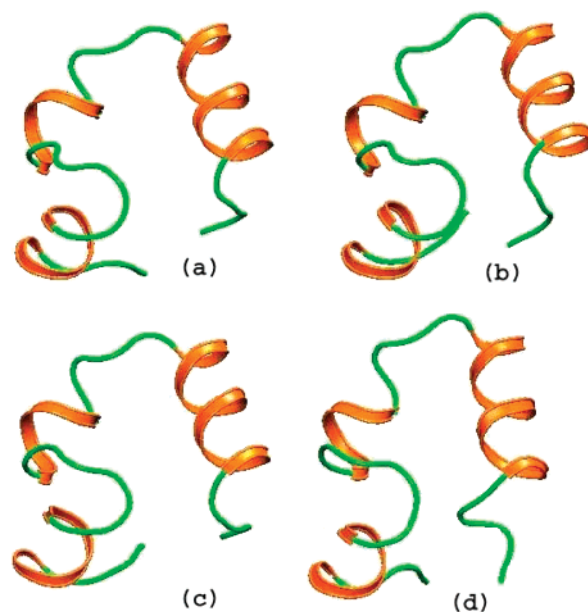


Figure 2. Snapshots of a few representative configurations of the protein in solution as obtained at (a) 1 ns, (b) 2 ns, and (c) 3.5 ns of the NVT simulation run. For comparison, the NMR structure³⁸ is also shown in (d). The protein coloring scheme is the same as in Figure 1.

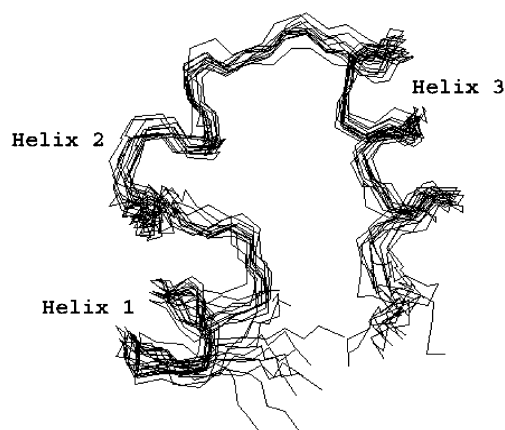


Figure 3. Superposition of the backbone N, C, and C $_{\alpha}$ atoms of 12 configurations taken at an interval of 200 ps from the equilibrated MD trajectory. The N-terminus is projected at the lower left, while the C-terminus is at the lower right.

minal secondary structures of the protein, particularly the three α -helices, are quite rigid, even in solution. Such rigidity of the solution structure is comparable to that observed experimentally as reported by McKnight et al.³⁸ The segments coil-1 and coil-4, being at the two ends of the protein, were found to be more flexible in nature.

To investigate in a quantitative manner the differences between the simulated and the native structures, we have calculated the RMSD between them. The RMSD is also an important quantity that can provide valuable insight into the local dynamics of the protein structure at a microscopic level. The RMSD values were calculated for all the non-hydrogen atoms of the protein molecule (backbone and the residue side chains) as well as for only the protein backbone atoms (N, C, and C $_{\alpha}$ atoms). For simplicity we denote the former as RMSD $_{\text{all}}$ and the latter as RMSD $_{\text{back}}$. In Figure 4 we display the variation of both the RMSD values with respect to time for the protein molecule. The average RMSD calculated over all the non-hydrogen atoms was found to be 2.72 Å, while that for the backbone atoms was 1.72 Å. The lesser values for RMSD $_{\text{back}}$

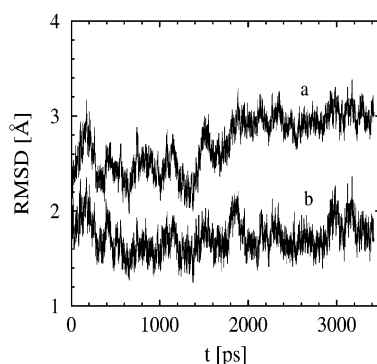


Figure 4. Time evolution of the RMSD of the simulated structure from the native state structure. The RMSD for all the non-hydrogen atoms (RMSD_{all}) and for only the backbone (N, C, and C_α) atoms ($\text{RMSD}_{\text{back}}$) are displayed as “a” and “b” respectively.

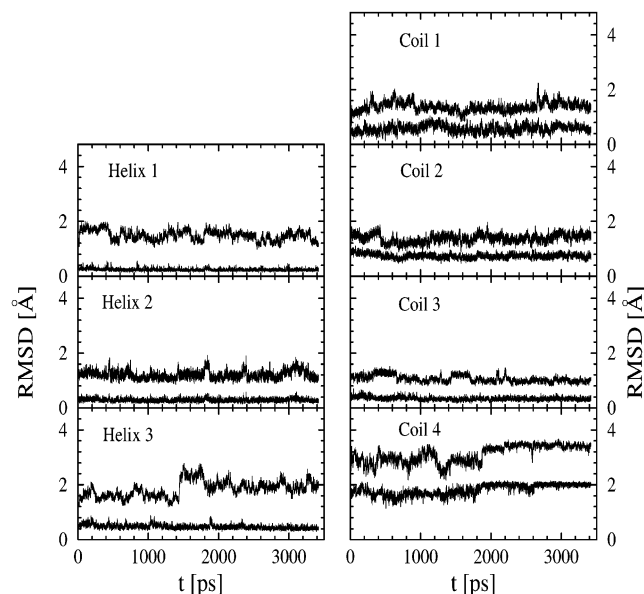


Figure 5. Time evolution of the RMSD of different secondary structures (three α -helices and four coils) from the corresponding native state structures. RMSD values for all the non-hydrogen atoms (RMSD_{all}) and the backbone atoms ($\text{RMSD}_{\text{back}}$) are drawn separately (“top” and “bottom” curves, respectively) for each case.

relative to RMSD_{all} are on expected lines because the side chain mobility contributes to the latter. An important feature to note from these RMSD plots is the presence of a small but noticeable jump in RMSD_{all} during the time interval 1400–1800 ps of the simulation run. The average value for the RMSD_{all} from 0 to 1700 ps was found to be 2.47 Å, while that for the rest of the simulated trajectory was 2.95 Å. This corresponds to an approximately 20% increase in RMSD_{all} in that time interval. It is also important to note that $\text{RMSD}_{\text{back}}$ did not show any such change during the time scale of the simulation. This may be an interesting observation that indicates that the side chains of some of the residues are probably undergoing oscillation from one conformational substate to another of the protein. Such transitions have been found in earlier experimental and computer simulation studies.³⁴

To understand such a behavior of the protein side chains in a more microscopic manner, we have separately calculated RMSD_{all} and $\text{RMSD}_{\text{back}}$ for the different segments of the protein (α -helices and coils) and display them in Figure 5. It is clear from the figure that for the helices 1 and 2 and coils 1–3, the motions are mainly featureless. It is also apparent from the variation of $\text{RMSD}_{\text{back}}$ that the backbones of the secondary

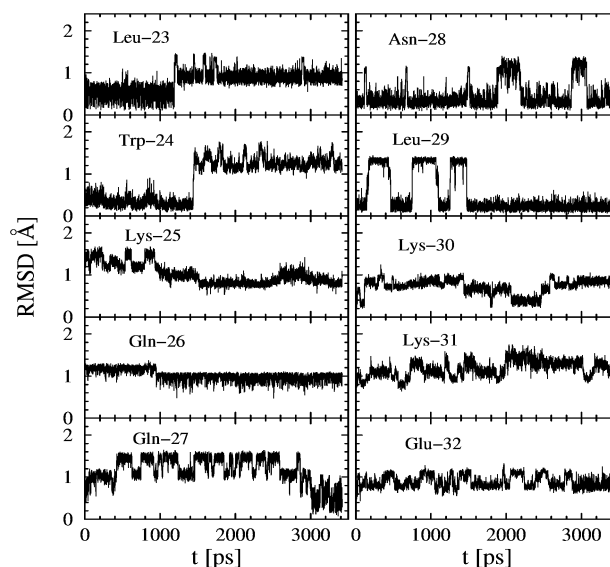


Figure 6. Time evolution of the RMSD_{all} of individual amino acid residues (Leu-23 to Glu-32) of α -helix-3.

structures, particularly those of the helices, are rigid and stable. This is in agreement with Figure 3. However, note the variation of RMSD_{all} for helix-3. There is a sharp jump in RMSD_{all} for helix-3 at around 1400 ps. The calculated average RMSD_{all} for helix-3 from 0 to 1400 ps was 1.6 Å, as against 2.0 Å, for the rest of the trajectory. This indicates a jump of 25% for the RMSD_{all} of helix-3. Besides, coil-4 also showed some oscillation in the RMSD values in the same part of the trajectory. However, those are much smaller compared to that of helix-3 and mainly arise because of its closeness to the C-terminus of the protein, which is quite flexible (see Figure 3). Such findings coupled with the fact that the backbones of all the nonterminal segments (helices 1–3 and coils 2 and 3) are significantly rigid indicate that the side chains of one or more residues of helix-3 may exhibit bistable motions in solution, which is manifested in the jump observed in RMSD_{all} for the entire protein molecule (see Figure 4). Such motions of the residues in helix-3 are significant from the point of view of the biological activity of HP-36 because several of the active site residues are located in helix-3.³⁸

To gain further insight and to identify the residues responsible for such interesting dynamics, we have examined the RMSD_{all} of each of the 10 amino acid residues of helix-3 (Leu-23 to Glu-32). These are shown in Figure 6. As expected, the backbone of each of the residues has been found to be quite rigid and hence not shown in the figure. However, the side chain motions of the residues show highly interesting dynamics. Several of them exhibit oscillatory motion. In particular, the hopping motion of the side chains of residues Leu-23 and Trp-24 is quite interesting. It is apparent that the side chains of these two residues exist in two conformational states within the time scale of the simulation. Transition from one state to the other is accompanied by large-amplitude motions, as evident from the jump in their RMSD_{all} values. In fact the separation between the two states is so distinct in each case that these are reflected in the overall RMSD of helix-3, as well as in that of the whole protein molecule. Besides, some of the other residue side chains in helix-3 also demonstrate frequent large-amplitude oscillatory motions, which are often quasi-periodic (Leu-29) in nature. Such motions might involve conformational changes of the residues due to rotations of specific groups in the side chains. However, this needs to be investigated further. Such large-scale oscillations have also been seen in single-molecule spectroscopy^{50,51} and

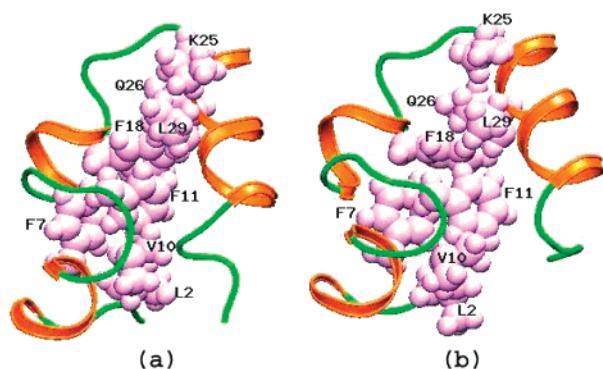


Figure 7. (a) Native state structure of the protein, highlighting the core amino acid residues.³⁸ Snapshot of the structure of the protein at the end of the simulation, highlighting those core residues, is displayed in (b).

can provide important information about the microscopic motion of amino acid residues in a secondary structure of a protein.

It is also interesting to note that identical residues present in the same secondary structure, such as helix-3 in our case, can exhibit different local dynamics. This is clearly evident for residues Leu-23 and Leu-29 or Gln-26 and Gln-27. Such differences in side chain dynamics of similar residues are expected to arise from the difference in their locations along the helical turn and the latter's likely influence on the packing of the residue side chains toward the core of the protein. For example, in helix-3, the residues Gln-26 and Leu-29 are packed along the helix in such a fashion that they remain significantly buried in the hydrophobic core of the protein. As a result, the side chains of these two residues have less freedom to move. This is reflected in the relatively quiet nature of their dynamics with some occasional sharp jumps (Leu-29), compared to either more frequent oscillatory motion of Gln-27 or less frequent long time scale two-state motion of Leu-23 side chains, which are not located toward the core. Such relatively less noisy side chain motions are also observed for other core residues located in other secondary structures (figures not shown). In Figure 7 we highlight the core amino acid residues of the native state NMR structure of HP-36³⁸ along with a configuration obtained from our simulation. Our study reveals that the side chain orientation of most of the core residues except Leu-2, which is near the N-terminus, remain quite similar during the time scale of the simulation compared with that observed in experiments. It is important to note that helix-3 contains several residues (Lys-25, Lys-30, Lys-31, Glu-32) that are active sites for actin binding.³⁸

3.2. Water Structure at the Protein Surface. It is believed that the structure and dynamics of water around the secondary structures of a protein molecule can play a crucial role in determining its biological activity. We have shown in the previous section that the amino acid residues in helix-3 exhibit considerable motion in the native state. Helix-3 also contains several active sites that take part in the actin binding process. It would therefore be interesting to investigate in detail the structure of water molecules around helix-3 and compare that with the water structure around other similar secondary structures within the protein molecule, namely, helices 1 and 2, which do not contain any active site. With this aim, we have calculated the pairwise correlation function, commonly known as the radial distribution function, $g(r)$, of the water molecules with the backbone C_α atoms of the residues belonging to each of the three helices and presented in Figure 8. The distribution functions show interesting structural behavior of the water molecules around the three helices. It is clear that the water

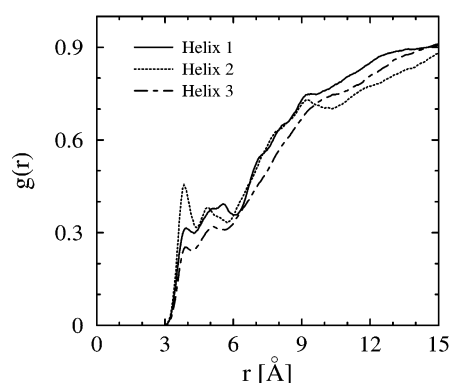


Figure 8. Pairwise correlation function, $g(r)$, of water molecules as a function of distance from the C_α atoms belonging to the three α -helices.

near helix-2 is most structured among the three helices, with a sharp peak around 4 Å. The function for helix-2 also exhibits a distinct second peak at 5 Å. Interestingly, the intensity of the first peak for both helix-1 and helix-3 is much less compared to that for helix-2. In fact, this first peak has almost disappeared for helix-3. The intensity of the second peak is also much lower for helix-3. This indicates clearly that the water around helix-3 is the least structured among all three helices. Such a lack of water structure around helix-3 is an important observation. Let us explain the reason behind this observation. There are three factors on which the intensity of the distribution function and hence the structure of water around the helices are likely to depend. These are (i) the fraction of amino acid residues with long side chains, (ii) the relative hydrophilicity and hydrophobicity of the residues, and (iii) the motion of the residue side chains. There is not much difference in the fraction of residues with long side chains, particularly between the helices 1 and 3. About 60–70% of the residues in these two helices contain long side chains, while $\sim 50\%$ of the residues in helix-2 have long side chains. Thus, we believe that the size of the residue side chains may not have much influence on the structure of water around the helices. From the *hydropathy scale* of amino acid residues,⁵² we have calculated the average hydropathy per residue for the three helices. The calculated values are -2.32 , -0.18 , and -1.90 for helices 1, 2, and 3, respectively. This indicates that helix-2 is the least hydrophilic among the three helices. Thus, on this basis, one would expect the least ordering of water around helix-2. However, the reverse has been found to be true. Therefore, the structure of water around the three helices cannot be explained by their relative hydrophilic–hydrophobic nature alone. However, the lack of water structure around helix-3 agrees nicely with large-amplitude oscillations or hoppings noticed for the side chain motions of its residues (see Figure 6). Such large-amplitude motion of residue side chains in helix-3 prevent ordering of water around it, which is reflected in the corresponding $g(r)$ curve. The ordering of water around helix-2 is consistent with low-amplitude steady oscillations of the corresponding amino acid residue side chains (see Figure 5). The results for helix-3 also correlate well with the biological activity of the protein molecule. It is expected that for successful binding activities, the water around the active sites should be less structured. This is precisely what we observe for helix-3, which, as mentioned earlier, contains several active residues that take part in the function of the protein.

3.3. Dynamics of Water at the Interface. The significantly different water structure around the three α -helices (discussed in the previous section) should affect both translational and reorientational dynamics of water near the helices, which in turn

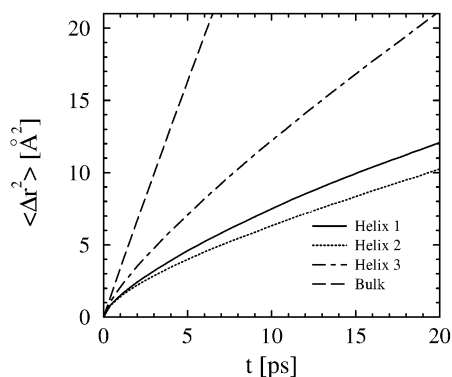


Figure 9. Mean square displacement (MSD) of the water molecules near the three α -helices. Water molecules that reside within 5 Å from an atom belonging to the residues in the respective helices are considered. The MSD of the water molecules present in the bulk is also shown for comparison.

is likely to influence the biological activity of HP-36. In this section, we discuss the dynamics of water.

3.3.1. Translational Motion of the Surface Water. It is well-known that the mobility of individual water molecules near the surface of a protein shows different dynamical behaviors, which range from “bound” water to “mobile” water diffusion at the protein surface.^{21,22} The mobility of water molecules can be studied by calculating the diffusion coefficients (D) from the slope of the mean square displacement vs time curve, using the well-known Einstein’s relation⁴⁹

$$D = \lim_{\Delta t \rightarrow \infty} \frac{\langle |\mathbf{r}_i(t) - \mathbf{r}_i(0)|^2 \rangle}{2d\Delta t} = \lim_{\Delta t \rightarrow \infty} \frac{\langle \Delta r^2 \rangle}{2d\Delta t} \quad (1)$$

where d is the dimensionality of the system, $\mathbf{r}_i(t)$ and $\mathbf{r}_i(0)$ are the coordinates of the i th water molecule at time t and at time 0, respectively, and the averaging is over both time origins and water molecules.

We have calculated the mean square displacement of water molecules that are in proximity to the three α -helices. To be specific, we have performed the calculation for those water molecules that reside within 5 Å from any atom of the residues belonging to each of the helices. These are shown in Figure 9. For comparison we have also displayed the same for the bulk water. The bulk water molecules are defined as those that reside beyond 25 Å from the protein atoms. It is clear that the translational diffusion of water molecules is much restricted near the protein surface. Such restricted mobility of water near the surface of a heterogeneous macromolecule is well-known.^{21,22,53} However, the most interesting feature to note from the figure is that the mobility of water molecules near the three α -helices are significantly different from one another. It is evident that the water molecules around helix-3 are more mobile than those around the other two helices. We have calculated the diffusion coefficient (D) values from the mean square displacement data corresponding to the three helices in the time interval 10–20 ps using eq 1. These values are listed in Table 1. The data show that the water molecules within the hydration layer of the helices are 3–7 times slower than the bulk water. However, within the hydration layer, the water molecules around helix-3 are almost 1.9–2.3 times more mobile than those around the other two helices. Such higher translational mobility of water near helix-3 agrees well with the lower ordering of water around it, as observed in the previous section. At this point, we emphasize that the absolute values of the diffusion coefficients may not be very authentic for water molecules close to the protein

TABLE 1: Diffusion Coefficients of the Water Molecules around the Three α -Helices of the Protein, As Obtained from Their Mean Square Displacements^a

segment	D ($10^{-5} \text{ cm}^2 \text{ s}^{-1}$)
helix-1	0.76
helix-2	0.65
helix-3	1.48
bulk water	4.74

^a The value for bulk water is also listed for comparison.

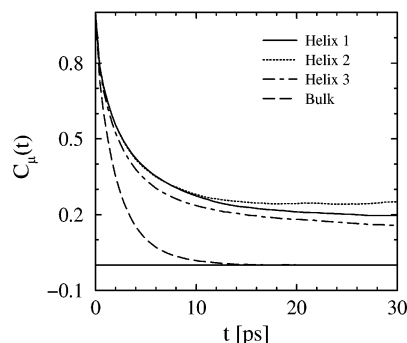


Figure 10. Reorientational time correlation function of the water dipoles, $C_\mu(t)$, for the water molecules in proximity to the three α -helices of the protein. The TCF for the water molecules present in the bulk is also shown for comparison.

surface. This is because it was shown recently that water near a protein surface show a sublinear trend in the variation of their mean square displacements with time.^{21,22} However, here we are interested in the relative diffusion of water within the hydration layer of different segments of the protein molecule rather than the calculation of the absolute diffusion coefficient values.

3.3.2. Orientational Motion of the Surface Water. In a solution containing a heterogeneous macromolecule (such as protein), the reorientational dynamics of water molecules near the macromolecular interface is significantly affected. Within the framework of the linear response theory, the reorientational motion of water at an interface can be studied by dielectric relaxation experiments. The rotational motion of water can be investigated by measuring the reorientational dynamics of its electrical dipole $\vec{\mu}$, defined as the vector connecting the oxygen atom of the water molecule to the center of the line connecting the two hydrogen atoms. The time evolution of $\vec{\mu}$ can be estimated by measuring the dipole–dipole time correlation function (TCF), defined as

$$C_\mu(t) = \frac{\langle \hat{\mu}_i(t+\tau) \cdot \hat{\mu}_i(\tau) \rangle}{\langle \hat{\mu}_i(\tau) \cdot \hat{\mu}_i(\tau) \rangle} \quad (2)$$

where $\hat{\mu}_i(t)$ is the unit dipole moment vector of the i th water molecule at time t and the angular brackets denote averaging over the water molecules and over initial times τ .

Again, we restrict ourselves to the reorientational motion of the water molecules that are in proximity to the three α -helices (i.e., within 5 Å from the atoms in the helices). The correlation functions were calculated by averaging over these water molecules only. In Figure 10 we show the variation of $C_\mu(t)$ against time for the water molecules near the three helices. For comparison, we have also shown the relaxation for the bulk water. It is clearly evident from the figure that the water molecules around helix-3 reorient noticeably more quickly than those around helix-1 and helix-2. This once again agrees with the reduced water structure around helix-3 (discussed earlier).

TABLE 2: Multiexponential Fitting Parameters for the Dipolar Time Correlation Functions of Water Molecules around the Three α -Helices of the Protein^a

segment	time constant (ps)	amplitude (%)	$\langle\tau_{\mu}\rangle$ (ps)
helix-1	0.43	25.0	33.16
	4.14	50.5	
	126.37	24.5	
helix-2	0.35	22.0	17.07
	3.68	53.7	
	large	24.3	
helix-3	0.31	20.4	2.03
	3.03	54.4	
	60.94	25.2	
bulk water	0.36	21.3	2.03
	2.48	78.7	

^a Corresponding parameters for bulk water are also listed for comparison. $\langle\tau_{\mu}\rangle$ is the average time constant.

Exhibition of faster dipolar reorientational motion of water near helix-3 correlates nicely with the presence of active sites taking part in the actin binding process. The extraordinary slow decay for the helix-2 (manifested in a nearly flat decay curve) is found to be due to the presence of a small fraction of *quasi-bound* water molecules near the surface of the helix. We have earlier found a similar correlation between faster water dynamics and biological activity for the pathogenic stain of enterotoxin, 1ETN.³¹ While it is tempting to imagine the existence of such a correlation based on simulation results, one should note that the signature, while noticeable, is not overwhelming. Therefore, it is not clear how much of a role this faster water dynamics can play in molecular recognition and ligand binding. Probably more striking is the large-amplitude motion of the amino acid residues in helix-3. But again, much more work is needed to pin down the origin and the connection with biological activity.

It is also important to understand the observed time correlation functions in a more quantitative way by estimating the time scales associated with them. We notice that even though the water molecules around helix-3 reorient more quickly compared to those around the other two helices, all the curves show slower decay at long times. Such long-time decay cannot be described by a single-exponential law. One can fit such functions to a multiexponential form.^{31,53} It is a common practice to use multiexponentials because one can then directly obtain time constants associated with different motions. Here, we have used a sum of three exponentials to fit the data for each of the three TCFs. The parameters for best fit are shown in Table 2. Water molecules around helix-2 exhibit significantly slower dynamics with a long time component, which we could not determine because of the limitation of the time scale of our simulation. Similar behavior has also been observed recently by us for a smaller protein, enterotoxin.³¹ As discussed above, the existence of such a long time component arises because of particular water molecules that are “bound” to specific residues in helix-2. However, we need to investigate this aspect further. One can note that the average reorientational motion of water molecules around helix-3 is almost twice faster compared to that for water around helix-1. This is due to the presence of a long time component of about 126 ps for water around helix-1, which is more than twice longer than the corresponding long time component for helix-3. It is also noted that the reorientation of water molecules in bulk ($\langle\tau_{\mu}\rangle = 2$ ps) is much faster than the water molecules near any of the three helices. From our results it is clear that even though the rotational motion of water at the interface of a protein is much slower compared to that of bulk water, distinct differences might arise in different regions of the interface containing almost identical secondary structures,

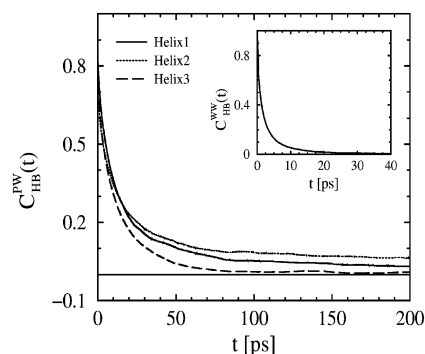


Figure 11. Time correlation function $C_{HB}^{PW}(t)$ for the hydrogen bonds formed between the amino acid residues of the three α -helices of the protein and the interfacial water molecules. The inset shows the same for the hydrogen bonds formed between water molecules present in the bulk.

such as three α -helices in HP-36. To obtain a microscopic understanding of such differential dynamics and its likely influence on the binding activity of the protein, it would be interesting to study the properties of the hydrogen bonds formed between the interfacial water molecules and the protein. This is discussed in the next section.

3.4. Hydrogen Bond Analysis. The structural organization and dynamics of the interfacial water molecules are also coupled with the protein residues by a network of hydrogen bonds formed between them.^{22,54–57} The formation and breaking of these hydrogen bonds play an important role in determining the functionality of the protein. One can use either a geometric^{22,55,58} or an energetic^{59,60} criterion to define a hydrogen bond. In this work, we have employed a purely geometric criterion to define a hydrogen bond.⁵⁸

The structural relaxation of hydrogen bonds can be characterized by the time correlation function,

$$C_{HB}(t) = \frac{\langle h(t+\tau) h(\tau) \rangle}{\langle h \rangle} \quad (3)$$

where the hydrogen bond population variable $h(t)$ is unity when a particular pair of protein–water or water–water sites is hydrogen-bonded at time t according to the definition used and is zero otherwise.^{27,61–67} The angular brackets denote averaging over all protein–water or water–water hydrogen bonds and over initial times τ . The correlation function $C_{HB}(t)$ describes the probability that a particular protein–water or water–water hydrogen bond is intact at time $t + \tau$, given it was intact at time τ . Thus, $C_{HB}(t)$ allows re-formation of a bond that is broken at some intermediate time. In other words, it allows recrossing the barrier separating the bonded and nonbonded states. Therefore, the relaxation of $C_{HB}(t)$ provides information about the structural relaxation of a particular hydrogen bond.

We have calculated the time correlation function $C_{HB}^{PW}(t)$ for the hydrogen bonds formed between the amino acid residues and the water molecules separately for the three helices of the protein molecule. These are displayed in Figure 11. The inset of the figure shows the corresponding function $C_{HB}^{WW}(t)$ for bulk water. These calculations are carried out by averaging over different sections of the trajectory with a time resolution of 16 fs. It is apparent from the figure that the structural relaxation of the protein–water hydrogen bonds is much slower than that of the water–water hydrogen bonds. However, the most interesting observation from this figure is the differences in the relaxation behavior of $C_{HB}^{PW}(t)$ for the three helices. The structural relaxation of the hydrogen bonds formed between the

residues in helix-3 and the interfacial water molecules is faster than that for the other two helices. This is an important result and agrees nicely with the faster, long-time diffusion and orientational relaxation of water molecules around helix-3, as discussed before. It also correlates well with the biological functionality of the protein because most of the active site residues in HP-36 are centered in helix-3. Currently, we are investigating the properties of protein–water and water–water hydrogen bonds at the interface of the protein in greater detail.

4. Conclusions

Let us first summarize the main results of this paper. In this article, we have presented results of an extensive atomistic MD simulation study of the structure and dynamics of aqueous chicken villin headpiece subdomain containing 36 amino acid residues (HP-36). The calculations revealed that although the simulated overall structure of the protein in solution remains quite similar to the native NMR structure, several interesting features in the local dynamics of the protein residue side chains could be observed. We noticed that within the time scale of the present simulation, many of the residue side chains in helix-3 undergo large-amplitude oscillatory motions. In particular, it is observed that for residues Leu-23 and Trp-24, the motions occurred between two well-defined states during the simulation. This could be important because helix-3 contains several actin binding sites. We have found that such large-amplitude oscillations in helix-3 influence the structure and dynamics of the water surrounding it. A reduced structuring of water molecules around helix-3 was noticed, as against that around the other two helices. Both translational and reorientational motion of the interfacial water were found to be slower compared to the bulk water. Interestingly, significant differences were observed among the interfacial water, near different segments of the protein. The most noticeable feature was that both translational and reorientational motions of water molecules within the hydration layer surrounding helix-3 were faster compared to those in the hydration layer of the other two helices. The structural relaxation of the hydrogen bonds formed between the amino acid residues in helix-3 and the surrounding water molecules was found to be faster than that for the other two helices. This was in agreement with the faster dynamics of the water molecules within the hydration layer of helix-3. These are interesting observations and may have important consequences on the biological activity of HP-36. Helix-3 of HP-36 hosts several active amino acid residues. Our observations indicate that low structuring of water coupled with their fast translational and reorientational motions near helix-3 may facilitate the binding process with actin. Similar behavior on differential water dynamics near an active site in the small protein enterotoxin has been observed earlier.³¹

Thus, in this work we have attempted to establish a correlation between three factors: (a) the biological activity of HP-36, (b) the natural dynamics of the amino acid residues, and (c) the structure and dynamics of the hydration water around the biologically active sites. The last, in turn, depends on several factors. We have shown that the large-amplitude local motion of the amino acid residue side chains and the relaxation of protein–water hydrogen bonds have important roles to play to determine the structure and dynamics of water around the active sites. A more detailed investigation of the network of hydrogen bonds formed at the protein–water interface is essential for a proper understanding of the correlation between the biological function of a protein and the structure and dynamics of both the protein and the surrounding water molecules. However, there

could be other factors as well that might influence such coupling between the protein and the interfacial water molecules. For example, the spatial orientation and the side chain packing of particular amino acid residues in the secondary structures may lead to specific water–residue interactions and could be vital. Some of these aspects are under extensive investigation in our laboratory.

Acknowledgment. This study was supported in part by grants from the Department of Biotechnology (DBT), Council of Scientific and Industrial Research (CSIR), and the Department of Science and Technology (DST), Government of India. S.C. thanks CSIR for providing a scholarship.

References and Notes

- (1) Grant, E. H.; McClean, V. E. R.; Nightingale, N. R. V.; Sheppard, R. J.; Chapman, M. J. *Bioelectromagnetics* **1986**, 7, 151.
- (2) Pethig, R. *Annu. Rev. Phys. Chem.* **1992**, 43, 177.
- (3) McCammon, J. A.; Gelin, B. R.; Karplus, M. *Nature* **1977**, 267, 585.
- (4) Bagchi, B. *Annu. Rep. Prog. Chem., Sect. C: Phys. Chem.* **2003**, 99, 127.
- (5) Nandi, N.; Bhattacharyya, K.; Bagchi, B. *Chem. Rev.* **2000**, 100, 2013.
- (6) Nandi, N.; Bagchi, B. *J. Phys. Chem. B* **1997**, 101, 10954.
- (7) Jordinades, X. J.; Lang, M. J.; Song, X.; Fleming, G. R. *J. Phys. Chem. B* **1999**, 103, 7995.
- (8) Pal, S. K.; Mandal, D.; Sukul, D.; Sen, S.; Bhattacharyya, K. *J. Phys. Chem. B* **2001**, 105, 1438.
- (9) Vajda, S.; Jimenez, R.; Rosenthal, S. J.; Fidler, V.; Fleming, G. R.; Castner, E. W. *J. Chem. Soc., Faraday Trans.* **1995**, 91, 867.
- (10) Joo, T.; Jia, Y.; Yu, J. U.; Lang, M. J.; Song, X.; Fleming, G. R. *J. Chem. Phys.* **1996**, 104, 6089.
- (11) Fleming, G. R. *Proc. Natl. Acad. Sci. U.S.A.* **1998**, 95, 15161.
- (12) Mandal, D.; Sen, S.; Sukul, D.; Bhattacharyya, K. *J. Phys. Chem. B* **2002**, 106, 10741.
- (13) Dutta, P.; Sen, P.; Halder, A.; Mukherjee, S.; Sen, S.; Bhattacharyya, K. *Chem. Phys. Lett.* **2003**, 377, 229.
- (14) Mukherjee, S.; Sen, P.; Halder, A.; Sen, S.; Dutta, P.; Bhattacharyya, K. *Chem. Phys. Lett.* **2003**, 379, 471.
- (15) Bhattacharyya, K. *Acc. Chem. Res.* **2003**, 36, 95.
- (16) Chagnon-Berret, P.; Choma, C. T.; Gooding, E. F.; DeGrado, W. F.; Hochstrasser, R. M. *J. Phys. Chem. B* **2000**, 104, 9322.
- (17) Pal, S. K.; Peon, J.; Bagchi, B.; Zewail, A. H. *J. Phys. Chem. B* **2002**, 106, 12376.
- (18) Pal, S. K.; Peon, J.; Zewail, A. H. *Proc. Natl. Acad. Sci. U.S.A.* **2002**, 99, 1763.
- (19) Sen, S.; Sukul, D.; Dutta, P.; Bhattacharyya, K. *J. Phys. Chem. A* **2001**, 105, 7495.
- (20) Rossky, P. J.; Karplus, M.; Rahman, A. *Biopolymers* **1979**, 18, 825.
- (21) Rocchi, C.; Bizzarri, A. R.; Cannistraro, S. *Phys. Rev. E* **1998**, 57, 3315.
- (22) Bizzarri, A. R.; Cannistraro, S. *J. Phys. Chem. B* **2002**, 106, 6617.
- (23) Tarek, M.; Tobias, D. J. *J. Am. Chem. Soc.* **1999**, 121, 9740.
- (24) Tarek, M.; Tobias, D. J. *Biophys. J.* **2000**, 79, 3244.
- (25) Tarek, M.; Tobias, D. J. *Phys. Rev. Lett.* **2002**, 88, 138101.
- (26) Marchi, M.; Sterpone, F.; Ceccarelli, M. *J. Am. Chem. Soc.* **2002**, 124, 6787.
- (27) Xu, H.; Berne, B. J. *J. Phys. Chem. B* **2001**, 105, 11929.
- (28) Lounnas, V.; Pettitt, B. M. *Proteins* **1994**, 18, 148.
- (29) Makarov, V.; Andrews, B. K.; Pettitt, B. M. *Biopolymers* **1998**, 45, 469.
- (30) Makarov, V.; Pettitt, B. M.; Feig, M. *Acc. Chem. Res.* **2002**, 35, 376.
- (31) Balasubramanian, S.; Bandyopadhyay, S.; Pal, S.; Bagchi, B. *Curr. Sci.* **2003**, 85, 1571.
- (32) Zhou, H. X.; Wlodek, S. T.; McCammon, J. A. *Proc. Natl. Acad. Sci. U.S.A.* **1998**, 95, 9280.
- (33) Duan, Y.; Kollman, P. A. *Science* **1998**, 282, 740.
- (34) Chen, L. X. Q.; Engh, R. A.; Brünger, A. T.; Nguyen, D. T.; Karplus, M.; Fleming, G. R. *Biochemistry* **1988**, 27, 6908.
- (35) Brooks, C. L., III; Grubbe, M.; Onuchic, J. N.; Wolynes, P. G. *Proc. Natl. Acad. Sci. U.S.A.* **1998**, 95, 11037.
- (36) Shoemaker, B.; Wolynes, P. G. *J. Mol. Biol.* **1999**, 287, 657.
- (37) Shoemaker, B.; Wang, J.; Wolynes, P. G. *J. Mol. Biol.* **1999**, 287, 675.
- (38) McKnight, C. J.; Matsudaira, P. T.; Kim, P. S. *Nat. Struct. Biol.* **1997**, 4, 180.
- (39) Doering, D. S.; Matsudaira, P. *Biochemistry* **1996**, 35, 12677.

- (40) Pope, B.; Way, M.; Matsudaira, P. T.; Weeds, A. *FEBS Lett.* **1994**, 338, 58.
- (41) McKnight, C. J.; Doering, D. S.; Matsudaira, P. T.; Kim, P. S. *J. Mol. Biol.* **1996**, 260, 126.
- (42) Tuckerman, M. E.; Yarne, D. A.; Samuelson, S. O.; Hughs, A. L.; Martyna, G. J. *Comput. Phys. Commun.* **2000**, 128, 333.
- (43) MacKerell, A. D., Jr.; Bashford, D.; Bellott, M.; Dunbrack, R. L., Jr.; Evanseck, J. D.; Field, M. J.; Fischer, S.; Gao, J.; Guo, H.; Ha, S.; Joseph-McCarthy, D.; Kuchnir, L.; Kuczera, K.; Lau, F. T. K.; Mattos, C.; Michnick, S.; Ngo, T.; Nguyen, D. T.; Prodhom, B.; Reiher, W. E., III; Roux, B.; Schlenkrich, M.; Smith, J. C.; Stote, R.; Straub, J.; Watanabe, M.; Wiorkiewicz-Kuczera, J.; Yin, D.; Karplus, M. *J. Phys. Chem. B* **1998**, 102, 3586.
- (44) Jorgensen, W. L.; Chandrasekhar, J.; Madura, J. D.; Impey, R. W.; Klein, M. L. *J. Chem. Phys.* **1983**, 79, 926.
- (45) Martyna, G. J.; Tuckerman, M. E.; Tobias, D. J.; Klein, M. L. *Mol. Phys.* **1996**, 87, 1117.
- (46) Darden, T.; York, D.; Pedersen, L. *J. Chem. Phys.* **1993**, 98, 10089.
- (47) Procacci, P.; Darden, T.; Marchi, M. *J. Phys. Chem.* **1996**, 100, 10464.
- (48) Procacci, P.; Marchi, M.; Martyna, G. J. *J. Chem. Phys.* **1998**, 108, 8799.
- (49) Allen, M. P.; Tildesley, D. J. *Computer Simulation of Liquids*; Clarendon: Oxford, 1987.
- (50) Hu, D.; Yu, J.; Barbara, P. F. *J. Am. Chem. Soc.* **1999**, 121, 6936.
- (51) English, D. S.; Harbron, E. J.; Barbara, P. F. *J. Phys. Chem. A* **2000**, 104, 9057.
- (52) Kyte, J.; Doolittle, R. F. *J. Mol. Biol.* **1982**, 157, 105.
- (53) Pal, S.; Balasubramanian, S.; Bagchi, B. *J. Chem. Phys.* **2002**, 117, 2852.
- (54) Hartsough, D. S.; Merz, K. M., Jr. *J. Am. Chem. Soc.* **1993**, 115, 6529.
- (55) Berendsen, H. J. C.; van Gunsteren, W. F.; Zwinderman, H. R. J.; Geurtsen, R. G. *Ann. N. Y. Acad. Sci.* **1986**, 482, 268.
- (56) Bizzarri, A. R.; Wang, C. X.; Chen, W. Z.; Cannistraro, S. *Chem. Phys.* **1995**, 201, 463.
- (57) Tirado-Rives, J.; Jorgensen, W. L. *J. Am. Chem. Soc.* **1990**, 112, 2773.
- (58) Reddy, C. K.; Das, A.; Jayaram, B. *J. Mol. Biol.* **2001**, 314, 619.
- (59) Mezei, M.; Beveridge, D. L. *J. Chem. Phys.* **1981**, 74, 622.
- (60) Stillinger, F. H.; Rahman, A. *J. Chem. Phys.* **1974**, 60, 1545.
- (61) Stillinger, F. H. *Adv. Chem. Phys.* **1975**, 31, 1.
- (62) Luzar, A.; Chandler, D. *Nature* **1996**, 379, 55.
- (63) Luzar, A.; Chandler, D. *Phys. Rev. Lett.* **1996**, 76, 928.
- (64) Chandra, A. *Phys. Rev. Lett.* **2000**, 85, 768.
- (65) Chandra, A. *J. Phys. Chem. B* **2003**, 107, 3899.
- (66) Balasubramanian, S.; Pal, S.; Bagchi, B. *Phys. Rev. Lett.* **2002**, 89, 115505.
- (67) Pal, S.; Balasubramanian, S.; Bagchi, B. *Phys. Rev. E* **2003**, 67, 061502.